

Stability Analysis of a Mathematical Model of Atherosclerotic Plaque Development: Fibrous Cap Formation and Degradation

Wanwarat Anlamlert¹, Yongwimon Lenbury^{1,*} and Jonathan Bell²

ABSTRACT

Atherosclerosis is an inflammatory disease in which plaque builds up in the artery wall. The growth of atherosclerotic plaque leads to the narrowing of the blood vessel, which may result in many possible disorders, such as coronary heart disease, cardiovascular diseases, myocardial infarction and stroke. This paper proposed a mathematical model of the essential chemical processes associated with atherosclerotic plaque development, which concentrates on the formation and possible degradation of the fibrous cap. It was shown that, under suitable conditions for the system parameters, the model system admits positive solutions. Local stability of the equilibrium was proven and conditions on the system parameters provided that ensure the system's global stability.

Keywords: atherosclerosis, atherosclerotic plaque growth, system stability, mathematical model, fibrous cap degradation

INTRODUCTION

Atherosclerosis is a disease usually located within the large arteries characterized by the formation of artery lesions which are the result of interactions between plasma molecules such as low density lipoproteins (LDL cholesterol), monocytes/ macrophages, cellular components and the extracellular matrix of the arterial wall and this process is referred to as plaque formation (Ross, 1999).

Normal arteries can cope with some blood vessel narrowing, as they are naturally larger than they need to be to achieve normal flow (Ross, 1999). Moreover, new blood vessels can often form to divert blood around problem areas. However, if the accumulation of LDL

cholesterol progresses further, atherosclerotic plaques will form leading to increasing numbers of proliferating smooth muscle cells and extracellular lipid. This can thicken the artery wall and interfere further with blood flow and stimulate further plaque formation (Ross, 1999). The growth of the plaques can become thrombotic and unstable, and rupture causing many serious disorders, such as coronary heart disease, cardiovascular diseases, myocardial infarction and stroke. Atherosclerosis overwhelmingly causes more morbidity and mortality in the world (Mathers and Loncar, 2006). The prevention and treatment of atherosclerosis is one of the most important problems in medicine. For this reason, better understanding of the atherosclerotic plaque development has been a subject of intense investigation.

¹ Department of Mathematics, Faculty of Science, Mahidol University, Rama 6 Road, and Centre of Excellence in Mathematics, CHE, 328 Si Ayutthaya Road, Bangkok 10400, Thailand.

² Department of Mathematics and Statistics, University of Maryland, Baltimore County, Baltimore, MD 21250, USA.

* Corresponding author, e-mail: scyllb@yahoo.com

In 2002, Cobbold *et al.* constructed a mathematical model of LDL oxidation *in vitro*. They studied the early stages of atherosclerosis which lead to the formation of the fatty streak. Their model is given by a system of ordinary differential equations governing the oxidation process within the context of an *in vitro* framework.

In 2010, Ibragimov *et al.* proposed a mathematical model of the early stage of atherosclerosis. They focused on the inflammatory components of the pathogenesis of cardiovascular disease (CVD). The concentrations of LDL, oxLDL, chemoattractant and the density of immune cells, smooth muscle cells (SMCs) and debris have been considered. Their model is given by a coupled system of non-linear reaction diffusion equations. They first presented some numerical simulations. The local stability analysis was then analyzed by decomposing the full system into two uncoupled problems.

In 2010, Calvez *et al.* constructed a mathematical model of atherosclerotic plaque initiation as a system of reaction-diffusion equations. They focused on the inflammatory process which takes place in the intima. Their model includes the cellular and chemical species in the intima: LDL, oxLDL, immune cells, foam cells, cytokines, and ECM. They proposed a one-dimensional model of lesion growth and then coupled their model with a blood flow satisfying Navier-Stokes equations in a two-dimensional domain. Numerical simulations were also given by using the finite element solver FreeFem++.

In 2012, the work of Bulelzai and Dubbeldam considered the effects of wall shear stress on the atherosclerotic plaque growth. They proposed a mathematical model consisting of four differential equations for the constituents of the plaque and also developed a second model in which the plaque evolution is coupled to the blood flow. Their models illustrated that both LDL-uptake and wall shear stress play important roles in the plaque development.

In the same year, Fok (2011) constructed a mathematical model of intimal thickening in atherosclerosis. This model represents a free boundary problem. Since the radius of the blood vessel lumen decreases due to the migration and proliferation of SMCs as time passes, the radius of the lumen was considered in this model. He analyzed the model and then compared the solutions with experimental data.

Recently, Hao and Friedman (2014) developed a mathematical model of the atherosclerotic plaque formation as a system of partial differential equations. In this work, they considered the interaction between LDL and high density lipoproteins (HDL) in the blood. Since HDL reduces the available free radicals in the blood, it reduces LDL transforming them into oxLDL, thus reducing the plaque growth. They showed that the various ratios of the concentration of LDL and HDL lead to the three different characteristics of plaque growth: high rise, low rise and non-rise of atherosclerosis.

The current study constructed a mathematical model of the late stages of atherosclerotic plaque formation which describes the fibrous cap formation and degradation. The model system admits positive solutions.

MODEL DERIVATION AND ANALYSIS

The concentration is considered of LDLs, L , oxidized LDLs, O , foam cells, F , oxidized LDL-derived chemoattractant G and macrophage-derived chemoattractant G_M , the density of macrophages, M , (SMCs), N , and extracellular matrix (ECM), K . Figure 1 provides a schematic diagram of the reactions among these components.

It was assumed that a constant source of LDL, σ , is supplied by the blood and that it is lost through the oxidation process by the reaction $L + R \rightarrow O$ with rate a_1 . The evolution of the LDL concentration is then governed by Equation 1:

$$\frac{dL}{dt} = \sigma - a_1RL, L(0) = L_0 \quad (1)$$

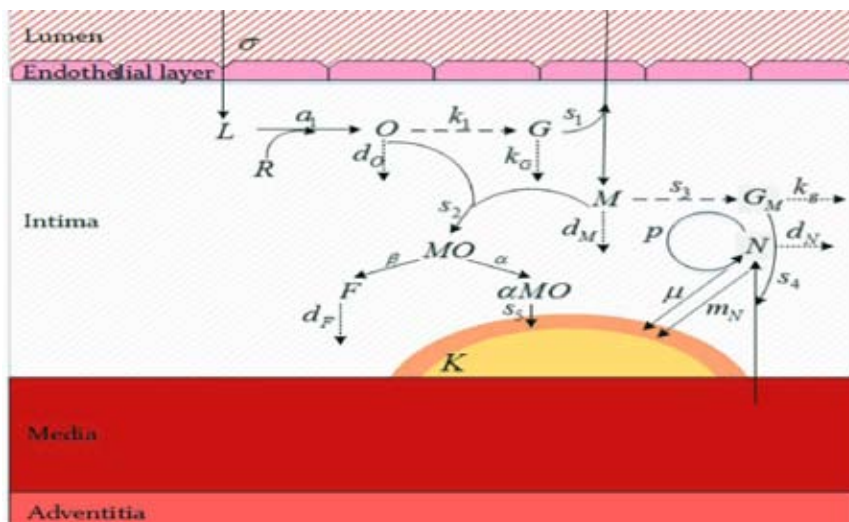


Figure 1 Schematic diagram of the network of reactions among the relevant components, as detailed in the text.

Oxidized LDL arises from LDL oxidation by a reaction with the free radicals R . It is reduced through ingestion by the macrophages and loss due to other processes as well as diffusion at the rate d_O . The oxidized LDL evolution is then described by Equation 2:

$$\frac{dO}{dt} = a_1RL - \frac{a_2MO}{(1+k_M M)(1+k_O O)} - d_O O, O(0) = O_0 \quad (2)$$

It was assumed that monocytes that migrate into the intima instantly mature into macrophages. The macrophages are recruited by the process involving oxidized LDLs, which are responsible for the production of a chemoattractant, G , for the macrophages. Equation 3 models the evolution of macrophages. Macrophages can be transformed into foam cells by the reaction $M + O \rightarrow F$, with the rate a_2 , and are reduced by natural death at the rate d_M .

$$\frac{dM}{dt} = s_2G - \frac{a_2MO}{(1+k_M M)(1+k_O O)} - d_M M, M(0) = M_0 \quad (3)$$

The evolution of foam cells, arising from the ingestion of oxidized LDLs by macrophages and reduced due to natural death at the rate d_F , is described by Equation 4:

$$\frac{dF}{dt} = \frac{\beta a_2 MO}{(1+k_M M)(1+k_O O)} - d_F F, F(0) = F_0 \quad (4)$$

While a portion of macrophages is transformed into foam cells at the fractional amount β , ($0 < \beta < 1$), the residual amount α will contribute to the formation of the fibrous cap. The model tracks two chemoattractants—one is due to the action of the oxidized LDLs and the other is derived from the macrophages. Equation 5 models the evolution of the first chemoattractant, G , which is an oxidized LDL-derived chemoattractant and can degrade at the rate d_G .

$$\frac{dG}{dt} = s_1O - d_G G, G(0) = G_0 \quad (5)$$

The second chemoattractant is a macrophage-derived chemoattractant necessary for the smooth muscle cells to enter the intima. This chemoattractant, the evolution of which follows Equation 6, can also be degraded at the rate d_g .

$$\frac{dG_M}{dt} = s_3M - d_g G_M - \frac{\rho G_M N}{1+k_g G_M}, G_M(0) = G_{M0} \quad (6)$$

It is assumed that SMCs can proliferate at the rate p and also degrade at the rate d_N . The migration of SMCs to the fibrous cap is included at the rate m_N ,

so that the extracellular matrix (ECM) components are produced. Equation 7 governs the smooth muscle cells evolution.

$$\frac{dN}{dt} = \frac{s_4 G_M}{1 + k_g G_M} + pN - m_N N - d_N N, N(0) = N_0 \quad (7)$$

Finally, Equation 8 models the evolution of ECM, which is remodeled by matrix metalloproteinase (MMP). Its amount depends on the proportions of macrophages and SMCs. Dead or damaged cells of the ECM are cleared at the rate d_K .

$$\frac{dK}{dt} = (m_N + \mu)N - \frac{\alpha a_2 s_5 KMO}{(1 + k_M M)(1 + k_O O)} - d_K K, K(0) = K_0 \quad (8)$$

In the above equations, $\alpha = 1 - \beta$, and all parameters are positive. The Hill type saturation functions are used for all the response terms in these equations, supported by experimental data reported by Kähler *et al.* (1997) and Hundal *et al.* (2001) and the work of Hao and Friedman (2014).

The following lemma shows that, under suitable conditions, all solutions of the system of Equations 1–8 are nonnegative. A set B in P_+^8 is identified such that all solutions starting from B remain bounded.

Lemma 1. *Let inequality (Equation 9),*

$$m_N + d_N > p \quad (9)$$

holds, and B be the region defined by

$$B = \left\{ (L, O, M, F, G, G_M, N, K) \in P_+^8 \mid \begin{aligned} &0 < L \leq \bar{L}, 0 < O \leq \bar{O}, 0 < M \leq \bar{M}, 0 < F \leq \bar{F}, \\ &0 < G \leq \bar{G}, 0 < G_M \leq \bar{G}_M, 0 < N \leq \bar{N}, 0 < K \leq \bar{K} \end{aligned} \right\}$$

where,

$$\bar{L} = \frac{\sigma}{a_1 R}, \bar{O} = \frac{\sigma}{d_O}, \bar{M} = \frac{\sigma s_1 s_2}{d_G d_M d_O}, \bar{F} = \frac{\beta a_2 \sigma^2 s_1 s_2}{d_F d_G d_M d_O^2},$$

$$\bar{G} = \frac{\sigma s_1}{d_G d_O}, \bar{G}_M = \frac{\sigma s_1 s_2 s_3}{d_g d_G d_M d_O},$$

Then, B is positive invariant and all solutions starting in B are bounded.

Proof. First, we show that a solution starting from within B is positive. Let $(L_0, O_0, M_0, F_0, G_0, G_{M0}, N_0, K_0) \in B$

Then, $L(t)$ would become non-positive if there existed a $t_0 > 0$ such that $L(t_0) = 0$ and $L(t) > 0$ for any $t, 0 \leq t < t_0$. Then, necessarily, $\left. \frac{dL}{dt} \right|_{t=t_0} \leq 0$ which is a contradiction because

$$\left. \frac{dL}{dt} \right|_{t=t_0} = \sigma - a_1 RL(t_0) = \sigma > 0.$$

Hence, $L(t)$ never vanishes and is positive for all $t_0 \geq 0$.

Next, $O(t)$ would become non-positive if there existed a $t_0 > 0$ such that $O(t_0) = 0$ and $O(t) > 0$ for any $t, 0 \leq t < t_0$. Then, necessarily, $\left. \frac{dO}{dt} \right|_{t=t_0} \leq 0$ which is a contradiction because

$$\begin{aligned} \left. \frac{dO}{dt} \right|_{t=t_0} &= a_1 RL(t_0) - \frac{a_2 M(t_0)O(t_0)}{(1 + k_M M(t_0))(1 + k_O O(t_0))} \\ &- d_O O(t_0) = a_1 RL(t_0) > 0. \end{aligned}$$

Hence, $O(t)$ never vanishes and is positive for all $t_0 \geq 0$.

$G(t)$ would become non-positive if there existed a $t_0 > 0$ such that $G(t_0) = 0$ and $G(t) > 0$ for any $t, 0 \leq t < t_0$. Then, necessarily, $\left. \frac{dG}{dt} \right|_{t=t_0} \leq 0$ which is a contradiction because

$$\left. \frac{dG}{dt} \right|_{t=t_0} = s_1 O(t_0) - d_G G(t_0) = s_1 O(t_0) > 0.$$

Hence, $G(t)$ never vanishes and is positive for all $t_0 \geq 0$.

The proof for the remaining variables is omitted since it simply follows in a similar fashion as for the above. Each equation has a degradation/clearance term vanishing to zero, which prevents the corresponding variable becoming negative. Moreover, each variable can be shown to admit a $\lim(\sup)$, which makes each production term bounded in the equations. Consequently, the clearance terms are (at least) growing linearly with respect to the variables, so the derivatives become negative when the “state” is large. In the following,

the detail of such proofs is given for only the first few variables.

We consider the model system (Equations 1–8) with $(L_0, O_0, M_0, F_0, G_0, G_{M0}, N_0, K_0) \in B$. From Equation 1, we obtain

$$L(t) = L_0 e^{-a_1 R t} + \frac{\sigma}{a_1 R} (1 - e^{-a_1 R t}) \leq \bar{L} e^{-a_1 R t} + \bar{L} (1 - e^{-a_1 R t})$$

Hence,

$$L(t) \leq \frac{\sigma}{a_1 R} = \bar{L} \text{ and } \limsup_{t \rightarrow \infty} L(t) = \frac{\sigma}{a_1 R} = \bar{L}$$

From Equation 2, we have

$$\frac{dO}{dt} \leq a_1 R \bar{L} - d_O O = \sigma - d_O O.$$

Then,

$$O(t) \leq O_0 e^{-d_O t} + \frac{\sigma}{d_O} (1 - e^{-d_O t}) \leq \bar{O} e^{-d_O t} + \bar{O} (1 - e^{-d_O t}).$$

Hence,

$$O(t) \leq \frac{\sigma}{d_O} = \bar{O} \text{ and } \limsup_{t \rightarrow \infty} O(t) = \frac{\sigma}{d_O} = \bar{O}.$$

From Equation 5, we have

$$\frac{dG}{dt} \leq s_1 \bar{O} - d_G G = \frac{\sigma s_1}{d_O} - d_G G.$$

Then,

$$G(t) \leq G_0 e^{-d_G t} + \frac{\sigma s_1}{d_G d_O} (1 - e^{-d_G t}) \leq \bar{G} e^{-d_G t} + \bar{G} (1 - e^{-d_G t}).$$

Hence,

$$G(t) \leq \frac{\sigma s_1}{d_G d_O} = \bar{G} \text{ and } \limsup_{t \rightarrow \infty} G(t) \leq \frac{\sigma s_1}{d_G d_O} = \bar{G}$$

From Equation 3, we have

$$\frac{dM}{dt} \leq s_2 \bar{G} - d_M M = \frac{\sigma s_1 s_2}{d_G d_O} - d_M M.$$

Then,

$$M(t) \leq M_0 e^{-d_M t} + \frac{\sigma s_1 s_2}{d_G d_M d_O} (1 - e^{-d_M t}) \leq \bar{M} e^{-d_M t} + \bar{M} (1 - e^{-d_M t}).$$

Hence,

$$M(t) \leq \frac{\sigma s_1 s_2}{d_G d_M d_O} = \bar{M} \text{ and } \limsup_{t \rightarrow \infty} M(t) \leq \frac{\sigma s_1 s_2}{d_G d_M d_O} = \bar{M}.$$

The boundedness of the remaining variables can be proved in a similar manner, and is thus omitted. \square

Next, let $\bar{X}_* = (L_*, O_*, M_*, F_*, G_*, G_{M*}, N_*, K_*)$ be the equilibrium point of Equations 1–8 for which the rates of change of all variables vanish, so that

$$\begin{aligned} L_* &= \frac{\sigma}{a_1 R}, O_* = \frac{\sigma}{s_2 M_* + d_O}, \\ M_* &= \frac{-(\sigma d_G k_1 s_2 + d_G d_M d_O) + \sqrt{(\sigma d_G k_1 s_2 + d_G d_M d_O)^2 + 4\sigma d_G d_M k_1 s_1 s_2}}{2d_G d_M s_2}, \\ G_* &= \frac{\sigma k_1}{d_G (s_2 M_* + d_O)}, F_* = \frac{\sigma \beta k_1 s_2 M_*}{d_F (s_2 M_* + d_O)}, \\ G_{M*} &= \left(\frac{m_N + d_N - p}{s_4} \right) N_*, \\ N_* &= \frac{-k_g + \sqrt{k_g^2 + \rho s_3 s_4 M_*} / (m_N + d_N - p)}{2\rho}, \\ K_* &= \frac{\beta (m_N + \mu) N_*}{(\alpha a_2 s_5 d_F F_* + \beta d_K)}, \end{aligned}$$

and

$$\begin{aligned} A &= \frac{a_2 M_*}{(1 + k_M M_*)(1 + k_O O_*)^2} + \frac{a_2 O_*}{(1 + k_M M_*)^2 (1 + k_O O_*)} + d_M + d_O, \\ B &= \frac{a_2 d_M M_*}{(1 + k_M M_*)(1 + k_O O_*)^2} + \frac{a_2 d_O O_*}{(1 + k_M M_*)^2 (1 + k_O O_*)} + d_M d_O, \\ C &= \frac{a_2 s_1 s_2 O_*}{(1 + k_M M_*)^2 (1 + k_O O_*)}. \end{aligned}$$

The parameters are all positive and the factors under the square root signs are all positive provided the condition in Equation 9 holds. Therefore, it is straight forward to see that the positive equilibrium solution exists. In addition, because of the positive sign in the term under the square root signs, the other solution with the negative square root will give a negative solution, and therefore the above positive equilibrium is unique provided the condition in Equation 9 holds.

By using the Routh-Hurwitz criteria, the following result follows immediately.

Theorem 2. *If Equation 9 holds and the following inequality Equation 10,*

$$A(d_G^2 + d_G A + B) > C, \tag{10}$$

also holds then \bar{X}_ is locally asymptotically stable.*

Proof. The characteristic polynomial associated with the system (Equations 1–8) is

$$(a_1R + \lambda)(d_F + \lambda) \left(d_K + \frac{\alpha a_2 s_5 M_* O_*}{(1 + k_M M_*)(1 + k_O O_*)} + \lambda \right) (\lambda^2 + p_1\lambda + p_2) (\lambda^3 + q_1\lambda^2 + q_2\lambda + q_3) = 0$$

where

$$p_1 = \left(d_g + \frac{\rho N_*}{(1 + k_g G_{M*})^2} \right) + (m_N + d_N - p),$$

$$p_2 = \left(d_g + \frac{\rho N_*}{(1 + k_g G_{M*})^2} \right) (m_N + d_N - p) + \frac{\rho s_4 G_{M*}}{(1 + k_g G_{M*})^3},$$

$$q_1 = d_G + A,$$

$$q_2 = d_G A + B,$$

$$q_3 = d_G B + C,$$

We see that the first three eigenvalues

$$\lambda_1 = -a_1 R, \lambda_2 = -d_F, \lambda_3 = -d_K - \frac{\alpha a_2 s_5 M_* O_*}{(1 + k_M M_*)(1 + k_O O_*)}$$

are all negative. We now consider Equation 11:

$$\lambda^2 + p_1\lambda + p_2 = 0 \tag{11}$$

We see that

$$p_1 = \left(d_g + \frac{\rho N_*}{(1 + k_g G_{M*})^2} \right) + (m_N + d_N - p) > 0,$$

$$p_2 = \left(d_g + \frac{\rho N_*}{(1 + k_g G_{M*})^2} \right) (m_N + d_N - p) + \frac{\rho s_4 G_{M*}}{(1 + k_g G_{M*})^3} > 0,$$

since Equation 9 holds. Hence, the eigenvalues $\lambda_i, i = 4, 5$, which are solutions of Equation 11, also have negative real parts.

We next consider the polynomial Equation

$$12: \lambda^3 + q_1\lambda^2 + q_2\lambda + q_3 = 0 \tag{12}$$

We see that

$$q_1 = d_G + A > 0,$$

$$q_2 = d_G A + B > 0,$$

$$q_3 = d_G B + C > 0,$$

The Routh table for Equation 12 is

λ^3	1	q_2	0
λ^2	q_1	q_3	0
λ^1	$q_3 - q_1 q_2$	0	0
λ^0	$q_3(q_3 - q_1 q_2)$	0	0

By Equation 10, we have

$$q_1 q_2 - q_3 = (d_G + A)(d_G A + B) - (d_G B + C) = d_G^2 A + d_G A^2 + AB - C = A(d_G^2 + d_G A + B) - C > 0,$$

that is, $q_1 q_2 > q_3$. Therefore, the number of sign changes in the first column of the Routh table is zero, which means Equation 12 has no non-negative solutions.

Hence, by the Routh-Hurwitz criteria, the eigenvalues for $\lambda_i, i = 6, 7, 8$, which are solutions of Equation 12, also have negative real parts and so the equilibrium point \bar{X}_* is locally asymptotically stable. \square

Finally, we consider the global stability of the model system (Equations 1–7) proved in the following theorem. Equation 8 is not included in this discussion since K can continue to grow in normal circumstances, whatever the dynamics, because humans, hence plaques, have a finite lifespan. On the other hand, clinical data in general show the other components to settle towards equilibrium levels as time progresses if there were no external stimuli. The model should be shown to admit global stability qualitatively similar to clinically observed data.

Theorem 3. *If the following inequalities (Equations 13–18),*

$$2d_O \geq a_1 R + s_1 + \frac{a_2}{k_O} \tag{13}$$

$$2d_M \geq s_2 + s_3 + \frac{a_2}{k_M} \tag{14}$$

$$2d_F \geq \beta a_2 \left(\frac{1}{k_M} + \frac{1}{k_O} \right) \tag{15}$$

$$2d_G \geq s_1 + s_2 \tag{16}$$

$$2d_g \geq \frac{\rho}{k_g} + s_3 + s_4 \tag{17}$$

$$2(m_N + d_N - p) \geq \frac{\rho}{k_g} + s_4 \tag{18}$$

hold, then the equilibrium point $\bar{X}_ = (L_*, O_*, M_*, F_*, G_*, G_{M*}, N_*, K_*)$ of Equations 1–7 is globally asymptotically stable.*

Proof. Relying on Krasovskii’s method (Slotine and Li, 1991), we suppose $x_1 = L - L_*, x_2 = O -$

$O_*, x_3 = M - M_*, x_4 = F - F_*, x_5 = G - G_*, x_6 = G_M - G_{M*}, x_7 = N - N_*$. Then, with $\underline{x} = x_1, x_2, \dots, x_7$ (the system (Equation 1–7) can be written as in Equations 19–25:

$$\dot{x}_1 = -a_1 R x_1 \equiv f_1(\underline{x}) \tag{19}$$

$$\begin{aligned} \dot{x}_2 &= a_1 R (x_1 + L_*) - \frac{a_2 (x_2 + O_*) (x_3 + M_*)}{(1 + k_O (x_2 + O_*)) (1 + k_M (x_3 + M_*))} \\ -d_O (x_2 + O_*) &\equiv f_2(\underline{x}) \end{aligned} \tag{20}$$

$$\begin{aligned} \dot{x}_3 &= s_2 (x_5 + G_*) - \frac{a_2 (x_2 + O_*) (x_3 + M_*)}{(1 + k_O (x_2 + O_*)) (1 + k_M (x_3 + M_*))} \\ -d_M (x_3 + M_*) &\equiv f_3(\underline{x}) \end{aligned} \tag{21}$$

$$\begin{aligned} \dot{x}_4 &= \frac{\beta a_2 (x_2 + O_*) (x_3 + M_*)}{(1 + k_O (x_2 + O_*)) (1 + k_M (x_3 + M_*))} \\ -d_F (x_4 + F_*) &\equiv f_4(\underline{x}) \end{aligned} \tag{22}$$

$$\dot{x}_5 = s_1 x_2 - d_G x_5 \equiv f_5(\underline{x}) \tag{23}$$

$$\begin{aligned} \dot{x}_6 &= s_3 (x_3 + M_*) - d_g (x_6 + G_{M*}) - \frac{\rho (x_6 + G_{M*}) (x_7 + N_*)}{1 + k_g (x_6 + G_{M*})} \\ &\equiv f_6(\underline{x}) \end{aligned} \tag{24}$$

$$\dot{x}_7 = \frac{s_4 (x_6 + G_{M*})}{1 + k_g (x_6 + G_{M*})} - (m_N + d_N - p) (x_7 + N_*) \equiv f_7(\underline{x}) \tag{25}$$

The equilibrium point of the system (Equations 19–25) is $X^* = (x_1^*, x_2^*, x_3^*, x_4^*, x_5^*, x_6^*, x_7^*) = \bar{0}$. Let J be the Jacobian matrix of the system (Equations 19–25), that is $J = (a_{ij})$, where

$$a_{11} = -a_1 R, a_{21} = -a_1 R,$$

$$a_{22} = \frac{-a_2 (x_3 + M_*)}{(1 + k_O (x_2 + O_*))^2 (1 + k_M (x_3 + M_*))}$$

$$-d_O, a_{23} = \frac{-a_2 (x_2 + O_*)}{(1 + k_O (x_2 + O_*)) (1 + k_M (x_3 + M_*))^2}$$

$$a_{32} = \frac{-a_2 (x_3 + M_*)}{(1 + k_O (x_2 + O_*))^2 (1 + k_M (x_3 + M_*))},$$

$$a_{33} = \frac{-a_2 (x_2 + O_*)}{(1 + k_O (x_2 + O_*)) (1 + k_M (x_3 + M_*))^2} - d_M, a_{35} = s_2,$$

$$a_{42} = \frac{\beta a_2 (x_3 + M_*)}{(1 + k_O (x_2 + O_*))^2 (1 + k_M (x_3 + M_*))},$$

$$a_{43} = \frac{\beta a_2 (x_2 + O_*)}{(1 + k_O (x_2 + O_*)) (1 + k_M (x_3 + M_*))^2}, a_{44} = -d_F,$$

$$a_{52} = s_1, a_{55} = -d_G,$$

$$a_{63} = s_3, a_{66} = -d_g - \frac{\rho (x_7 + N_*)}{(1 + k_g (x_6 + G_{M*}))^2},$$

$$a_{67} = -\frac{\rho (x_6 + G_{M*})}{1 + k_g (x_6 + G_{M*})},$$

$$a_{76} = \frac{s_4}{(1 + k_g (x_6 + G_{M*}))^2}, a_{77} = -(m_N + d_N - p).$$

and the other entries not mentioned above are all zero. We define a Lyapunov function V as $V = f^{Tf}$ where $f = (f_1, f_2, \dots, f_7)$. It is easily seen that

$$V \rightarrow \infty \text{ as } \|\underline{x}\| \rightarrow \infty.$$

It remains for us to show that the matrix

$$F = J + J^T = \begin{pmatrix} 2a_{11} & a_{21} & 0 & 0 & 0 & 0 & 0 \\ a_{21} & 2a_{22} & a_{23} + a_{32} & a_{42} & a_{52} & 0 & 0 \\ 0 & a_{23} + a_{32} & 2a_{33} & a_{43} & a_{35} & a_{63} & 0 \\ 0 & a_{42} & a_{43} & 2a_{44} & 0 & 0 & 0 \\ 0 & a_{52} & a_{35} & 0 & 2a_{55} & 0 & 0 \\ 0 & 0 & a_{63} & 0 & 0 & 2a_{66} & a_{67} + a_{76} \\ 0 & 0 & 0 & 0 & 0 & a_{67} + a_{76} & 2a_{77} \end{pmatrix}$$

is negative definite, that is, the determinants $(-1)^k \det(F_k) > 0$ for $k = 0, 1, \dots, 6$, where F_k is the matrix obtained from F by deleting $7 - k$ rows and $7 - k$ columns of F . Thus, $F_7 \equiv F$. We know that Equation 26 holds:

$$\det(-F_7) = (-1)^7 \det(F_7) = -\det(F_7). \tag{26}$$

In the following, we will show that $\det(-F_7) > 0$. We note that $-F_7 = (b_{ij})$ has positive diagonal elements. We see that

$$|b_{11}| = 2a_1 R > a_1 R = \sum_{i \neq 1} |b_{ij}|.$$

$$|b_{22}| \geq 2d_O > a_1 R + \frac{a_2}{k_O} + s_1 > a_1 R +$$

$$\frac{a_2 O}{(1 + k_M M)^2 (1 + k_O O)} + s_1 = \sum_{i \neq 2} |b_{ij}| \text{ by (13)}$$

$$|b_{33}| \geq 2d_M > \frac{a_2}{k_M} + s_2 + s_3 > \frac{a_2 M}{(1 + k_M M)(1 + k_O O)^2}$$

$$+ s_2 + s_3 = \sum_{i \neq 3} |b_{ij}| \text{ by (14)}$$

$$|b_{44}| \geq 2d_F > \frac{\beta a_2}{k_M} + \frac{\beta a_2}{k_O} > \frac{\beta a_2 M}{(1 + k_M M)(1 + k_O O)^2} +$$

$$\frac{\beta a_2 O}{(1+k_M M)^2 (1+k_O O)} = \sum_{i \neq 4} |b_{ij}| \text{ by (15)}$$

$$|b_{55}| \geq 2d_G > s_1 + s_2 = \sum_{i \neq 5} |b_{ij}| \text{ by (16)}$$

$$|b_{66}| \geq 2d_g > s_3 + \frac{\rho}{k_g} + s_4 > s_3 + \frac{\rho G_M}{1+k_g G_M} +$$

$$\frac{s_4}{(1+k_g G_M)^2} = \sum_{i \neq 6} |b_{ij}| \text{ by (17)}$$

$$|b_{77}| \geq 2(m_N + d_N - p) > \frac{\rho}{k_g} + s_4 + m_N + \mu >$$

$$\frac{\rho G_M}{1+k_g G_M} + \frac{s_4}{(1+k_g G_M)^2} m_N + \mu = \sum_{i \neq 7} |b_{ij}| \text{ by (18)}$$

Then, according to Haynsworth (1960), we can define L_i and R_i such that the condition in Equation 27,

$$\begin{aligned} b_{ii} &= L_i + R_i, \\ L_i &\geq \sum_{j < i} |b_{ij}|, \\ R_i &\geq \sum_{j > i} |b_{ij}|. \end{aligned} \tag{27}$$

holds for $i = 1, 2, \dots, 7$ and for any L_i and R_i , the condition (Equation 27),

$$\sum_{k=0}^7 \left(\prod_{i=1}^k L_i \prod_{i=k+1}^7 R_i \right) \leq \det(-F_7) \leq \sum_{k=0}^7 \prod_{i=1}^{k-1} (L_i + 2R_i) L_k \prod_{i=k+1}^7 R_i \tag{28}$$

holds, where an empty product is defined to be 1. Since in all the rows of F_7 , at least one entry, that is not along the diagonal, is nonzero, the lower bound of $\det(-F_7)$ in Equation 28 is positive. Therefore, $\det(F_7) < 0$.

Now, if we delete the seventh row and seventh column of F_7 to obtain F_6 , the same inequalities (Equations 13–18) will also guarantee that $\det(F_6) > 0$. In the similar manner, it follows that deleting two last rows and two last columns, we shall have $\det(F_5) = -\det(-F_5) < 0$. Deleting the last three rows and columns, we have $\det(F_4) > 0$, and so on. That is, $(-1)^k \det(F_k) > 0$ for $k = 0, 1, \dots, 6$, and F is negative definite. Based on the Krasovskii’s method (Feijer and Paganini, 2009) the equilibrium point of Equations 1–7 is globally asymptotically stable. □

NUMERICAL SIMULATION

Numerical simulations of the model system were carried out using $\sigma = 2016$, $R = 0.2772$, $\beta = 0.5$, $a_1 = 1.520 \times 10^4$, $a_2 = 0.3024$, $k_M = 10^{-3}$, $k_O = 10^{-3}$, $k_g = 10^{-3}$, $d_M = 6.048$, $d_O = 6.048 \times 10^2$, $d_F = 0.605$, $d_G = 0.01$, $d_g = 0.01$, $d_N = 1.008$, $d_K = 0.5$, $m_N = 1.68$, $s_1 = 6.05 \times 10^3$, $s_2 = 10.12$, $s_3 = 0.1814$, $s_4 = 1.814$, $s_5 = 6$, $\rho = 7.5$, $\mu = 6.05$. With such parametric values, if $p < 2.688$ then the inequalities in Equations 9 and 10 hold. Therefore, the equilibrium point \bar{X}_* is asymptotically stable as seen in Figures 2 and 3.

The selection of some of these parameter values was guided by the work of Hao and Friedman (2014). The values of critical parameters had to be adjusted to satisfy the conditions in the corresponding lemma or theorem.

Figure 2 shows a numerical simulation of the system in Equations 1–8 where $p = 2.5$ and all the state variables are seen to converge to their respective equilibrium levels. The solution trajectory of $K(t)$ increases rapidly initially and then decreases, tending toward the steady state value K_* as time passes.

Figure 3 compares the simulated time courses of ECM $K(t)$ when $0.0045 \leq p < 2.688$ in which case the equilibrium point is stable. When p is small, the level of ECM drops to a very low level. This is the situation where the fibrous cap becomes very thin. Thin caps of vulnerable plaques have a higher percentage of macrophages than SMCs, while the reverse is true in stable plaques with thick caps.

Physically, if there is a $T > 0$ such that for some predetermined $\delta > 0$, $K(t)$ decreases to the point that $K(t) \leq \delta$, we would expect the plaque to ‘rupture’. The rupture of these vulnerable plaques is thought to be responsible for most fatalities. Almost 73% of deaths from myocardial infarction (heart attack) are caused by plaque rupture (Davies, 1992).

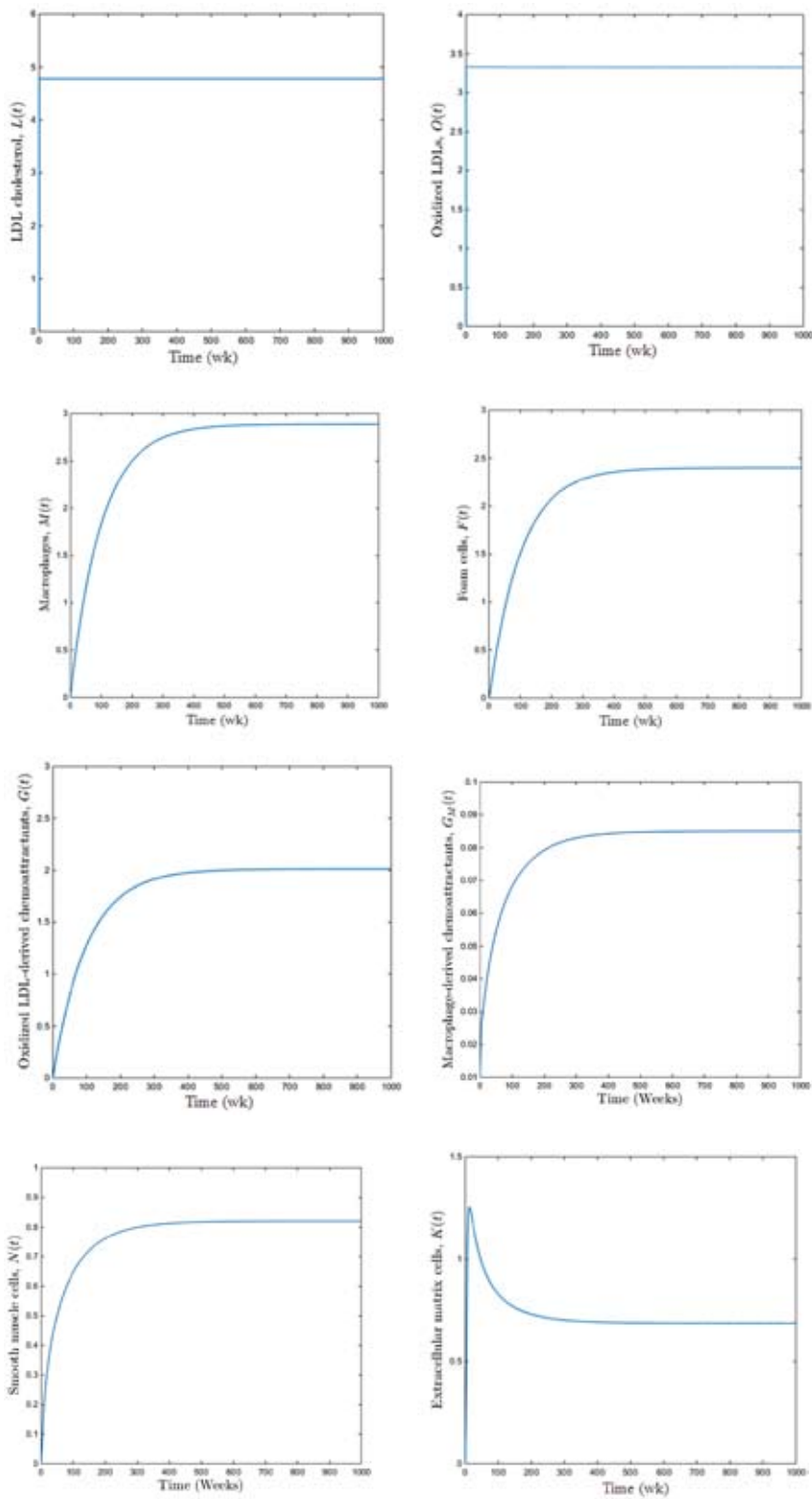


Figure 2 Computer simulation of the model system (Equations 1–8) with the parametric values given in the text and $p = 2.5$.

Some plaques remain stable throughout a person's life, though they can become of such size that they pose a health risk from stenosis (partial blockage of the artery, causing flow disruption). Such a situation is simulated by the model as seen

in Figure 4, where $p > 2.688$ and the conditions for stability are violated. The EMC level continues to grow, potentially giving rise to serious health complications in its turn.

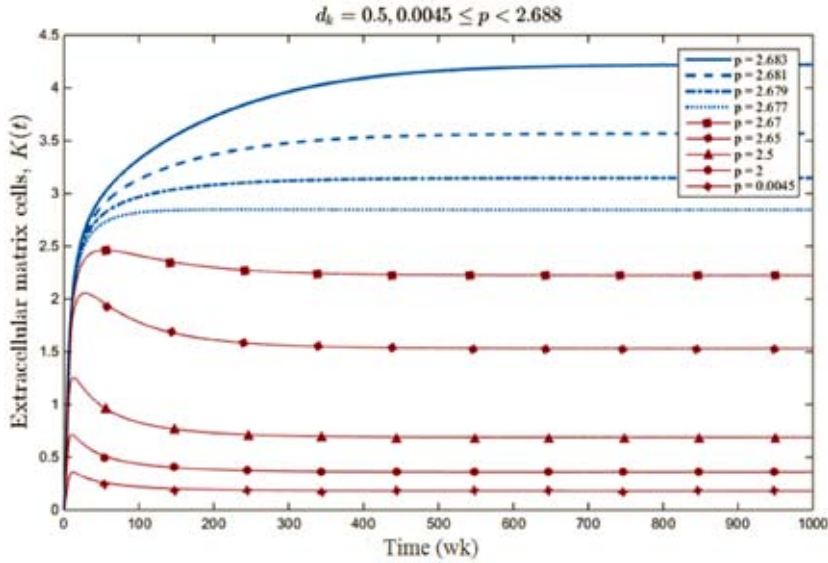


Figure 3 Computer simulation of the model system (Equations 1–8) with the parametric values given in the text and $0.0045 \leq p < 2.677$.

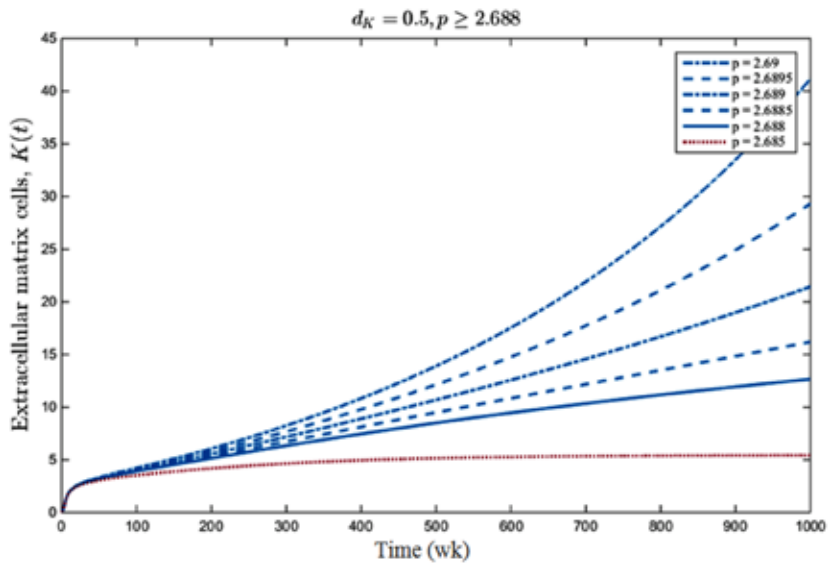


Figure 4 Computer simulation of the model system (Equations 1–8) with the parametric values given in the text and $p > 2.688$.

CONCLUSION

A model was constructed for atherosclerotic plaque development to describe the formation and degradation of the fibrous cap. Conditions were derived for the system parameters with all positive solutions being bounded. Local and global asymptotic stability were established. Finally, some numerical simulations were given to verify our theoretical predictions.

The model system can be globally stable under appropriate conditions. The stability of the equilibrium point \bar{X}_* , depends on the proliferation rate p of SMC, namely $N(t)$. If $m_N + d_N \leq p$, the system may change its behavior from being stable to unstable and the solution becomes unbounded which will impose stenosis on the lumen. However, this condition on the system parameters is only a sufficient condition for stability so that if it is violated, it may not necessarily mean that the system will become unstable.

Theorem 3 provides sufficient conditions for the global asymptotical stability property. It is possible that if one of the conditions (Equations 13–18) is violated, the system may still be globally stable. The “gap” between local asymptotic stability and global asymptotic stability is not due to the existence of multiple equilibria since the uniqueness of this is assured, but it could possibly be due to a development of oscillatory behavior. Further analysis on these points, specifically on how sharp the stability conditions are and the possibility of bifurcations to periodic solutions, are subjects of future research for possible further publication. This paper has focussed mainly on the stability property of the system because that is of major concern to the clinical profession—less so is the possibility of oscillatory behavior. Specifically, the atherosclerotic plaques are classified into two types: stable and vulnerable (unstable) plaque (Finn *et al.*, 2010), and the ability of the model to predict which type of plaque the physicians are dealing with is of crucial interest clinically.

Biologically, the condition in Equation 9 simply states that for the system to be stable, during which the components including the fibrous cap do not grow unboundedly causing health risks, the combined rate at which SMCs degrade and migrate to the fibrous cap should not exceed the rate at which it proliferates. The conditions in Equations 13–18 simply provide the lower bounds for the degradation rates of the respective components which ensure their stability, no matter how large or small their initial concentrations, running little or no risk of infarction.

The rate of cardiovascular disorder marked by coronary artery disease (CAD) is increasing in low-to-middle income countries including Thailand. The burden of CAD will have a significant impact on the healthcare system and the national budget. The prevention and treatment of atherosclerosis remain one of the most important problems in medicine.

ACKNOWLEDGEMENTS

Appreciation is extended to Mahidol University, Bangkok, Thailand and the Centre of Excellence in Mathematics, CHE, Thailand, for financial support.

LITERATURE CITED

- Bulelzai, M.A.K. and J.L. Dubbeldam. 2012. Long time evolution of atherosclerotic plaques. **J. Theor. Biol.** 297: 1–10.
- Calvez, V., J.G. Houot, N. Meunier, A. Raoult and G. Rusnakova. 2010. Mathematical and numerical modeling of early atherosclerotic lesions. *In* **ESAIM: Proceedings** 30: 1–14.
- Cobbold, C.A., J.A. Sherratt and S.R.J. Maxwell. 2002. Lipoprotein oxidation and its significance for atherosclerosis: a mathematical approach. **Bull. Math. Biol.** 64: 65–95.
- Davies, M.J. 1992. Anatomic features in victims of sudden coronary death. Coronary artery pathology. **Circulation** 85: 119–124.

- Feijer, D. and F. Paganini. 2009. Krasovskii's method in the stability of network control. In: **American Control Conference 2009**, Hyatt Regency Riverfront, St. Louis, MO, USA, 3292–3297.
- Finn, A.V., M. Nakano, J. Narula, F.D. Kolodgie and R. Virmani. 2010. Concept of vulnerable/unstable plaque. **Arterioscler. Thromb. Vasc. Biol.** 30: 1282–1292.
- Fok, P.W. 2012. Growth of necrotic cores in atherosclerotic plaque. **Math. Med. Biol.** 29: 301–327.
- Hao, W. and A. Friedman. 2014. The LDL-HDL profile determines the risk of atherosclerosis: a mathematical model. **PloS One.** 9: 1–15.
- Haynsworth, E.V. 1960. Bounds for determinants with positive diagonals. **Trans. Amer. Math. Soc.** 395–399.
- Hundal, R.S., B.S. Salh, J.W. Schrader, A. Gómez-Muñoz, V. Duronio and U.P. Steinbrecher. 2001. Oxidized low density lipoprotein inhibits macrophage apoptosis through activation of the PI 3-kinase/PKB pathway. **J. Lipid Res.** 42: 1483–1491.
- Ibragimov, A., L. Ritter and J.R. Walton. 2010. Stability analysis of a reaction-diffusion system modeling atherogenesis. **SIAM J. Appl. Math.** 70: 2150–2185.
- Kähler, C.M., P. Schratzberger and C.J. Wiedermann. 1997. Response of vascular smooth muscle cells to the neuropeptide secretoneurin a functional role for migration and proliferation in vitro. **Arterioscler. Thromb. Vasc. Biol.** 17: 2029–2035.
- Mathers, C.D. and D. Loncar. 2006. Projections of global mortality and burden of disease from 2002 to 2030. **PloS Med.** 3: 2011–2030.
- Ross, R. 1999. Atherosclerosis—an inflammatory disease. **N. Engl. J. Med.** 340: 115–126.
- Slotine, J.J.E. and W.P. Li. 1991. **Applied Nonlinear Control**. Prentice-Hall, Englewood Cliffs, NJ, USA.